Available online at www.sciencedirect.com
SCIENCE DIRECT®

Science Press

Trans. Nonferrous Met. Soc. China 17(2007) 1428−1432

Transactions of Nonferrous Metals Society of China

www.csu.edu.cn/ysxb/

Crystallography of Mg_2Sn precipitates in Mg-Sn-Mn-Si alloy

ZHANG Min(张 敏)[1], ZHANG Wen-zheng(张文征)[1], ZHU Guo-zhen(祝国珍)[1], YU Kun(余 琨)[2]

1. Laboratory of Advanced Materials, Department of Materials Science and Engineering, Tsinghua University, Beijing 100084, China;
2. Department of Materials Science and Engineering, Central South University, Changsha 410083, China

Received 15 July 2007; accepted 10 September 2007

Abstract: The microstructures of a Mg-Sn based alloy with trace additions of Mn and Si after various ageing heat-treatments were investigated. The alloy was found to contain mostly $Mg_2Sn(\beta)$ precipitates. The morphology and orientation relationships(OR) of Mg_2Sn precipitates were analyzed by using TEM. The Mg_2Sn precipitates mainly exhibit three shapes: lath, polygon and plate. Four ORs between Mg_2Sn precipitates and $Mg(\alpha)$ matrix are repeatedly detected, and two of them have never been reported before. Most of the lath-shaped β precipitates exhibit two OR. One is $(0001)_\alpha//(110)_\beta$, $[11\bar{2}0]_\alpha // [001]_\beta$ (OR-1), with the long axis along $[11\bar{2}0]_\alpha // [001]_\beta$; and the other is $(0001)_\alpha//(110)_\beta$, $[1\bar{1}00]_\alpha//[31\bar{1}]_\beta$ (OR-2, a new OR), with the long axis along $[1\bar{1}00]_\alpha//[31\bar{1}]_\beta$. The polygonal β exhibits $(0001)_\alpha//(111)_\beta$, $[2\bar{1}\bar{1}0]_\alpha//[\bar{1}10]_\beta$ (OR-3), with several pairs of facets. The plate-shaped β exhibits $(0001)_\alpha//(111)_\beta$, $[2\bar{1}\bar{1}0]_\alpha$ deviates by about 9° from $[\bar{1}10]_\beta$ (OR-4, a new OR).

Key words: Mg-Sn alloy; crystallography; Mg_2Sn precipitate; orientation relationship

1 Introduction

Magnesium alloys have drawn increasing attention in recent years. However, their strength restricts their further applications[1−2]. Numerous investigations have been carried out in searching for suitable Mg alloy systems with enhanced properties[3−6]. With the additions of rare earth elements, Mg alloys have shown improved properties both at room and elevated temperatures, but the high cost of rare earth elements has restricted their applications[7−9]. It is desirable to find other elements that might act similarly as RE elements according to the microstructures of Mg-RE systems. Based on examinations of the binary phase diagrams of Mg-X systems (X=metallic element), we found that Mg-Sn system has shown some promise to replace Mg-RE alloy. At the Mg-rich end of Mg-Sn phase diagram, there is a eutectic reaction with the eutectic temperature as high as 561 ℃, which is similar to Mg-RE systems, i.e. Mg-Nd (546 ℃) and Mg-Y (566 ℃) alloys. This temperature range is much higher than that of the most widely used Mg-Al and Mg-Zn systems. The high maximum solid solubility of Sn (14.5%, mass fraction) and the large variation of the solubility with temperature make the alloy a potentially effective age hardening system. However, only a limited number of investigations on Mg-Sn alloys have been reported in the past century[10−11]. It was reported that the precipitation process in Mg-Sn binary alloys involves solely the formation of equilibrium Mg_2Sn (β), and the orientation relationship(OR) between β and Mg matrix (α) varies with ageing temperature[10]. These β precipitates grow into laths or rods with the long axis along $[2\bar{1}\bar{1}0]_\alpha$ or plates parallel to $(0001)_\alpha$. According to NIE's analysis[12], this kind of morphology is not effective sufficiently for dispersion strengthening of precipitates in Mg alloys.

Recently, great efforts have been made on searching suitable alloying elements in Mg-Sn system, such as Al, Ca, Zn, In and Na[13−20]. However, the major precipitates remain to be Mg_2Sn. These additional trace elements has shown some effects, such as refining the precipitates and partly changing the morphology. Although

Foundation item: Projects(50471012; 50271035) supported by the National Natural Science Foundation of China
Corresponding author: ZHANG Wen-zheng; Tel: +86-10-62773795; E-mail: zhangwz@tsinghua.edu.cn

the morphology has not been changed significantly, the results have demonstrated the promising potential of improving mechanical properties.

Despite the recently renewed interest in Mg-Sn alloys, little progress was made on the crystallography of Mg_2Sn precipitates. Since the strengthening effect can be greatly affected by the crystallography of precipitates, it is worth examining the variation of crystallography corresponding to the composition change.

In the present study, Mn and Si were added into Mg-Sn binary system. The main reasons for choosing these two elements are: Mn is conventionally added into Mg-Al, Mg-Zn alloys to improve the corrosion resistance in the extent of about 0.1% (mass fraction), and Si is often added into Mg alloys to improve the high temperature strength. In addition, Mn-Si and Mn-Sn systems contain various compounds according to their binary phase diagrams. Thus it is interesting to investigate the microstructure of Mg-Sn-Mn-Si alloys, and to study the effect of Mn and Si on the precipitation behavior of Mg_2Sn, and also to examine possible existence of other precipitated phases.

2 Experimental

The alloy ingots were prepared by induction melting using steel crucibles and by casting into iron moulds. The chemical composition of the alloy is Mg-5.29%Sn-0.29%Mn-0.22%Si (mass fraction). The ingots embedded in MgO and C powder were homogenized at 520 ℃ for 48 h, and then water quenched. Artificial aging treatment was performed at 250 ℃ for various time periods. The age hardening responses were measured by micro-hardness tester under a load of 1.96 N. Specimens for TEM were twin-jet electro-polished in a solution containing 5 g lithium chloride, 11 g magnesium chlorate, 500 mL methanol and 100 mL 2-butoxy-ethanol, at −50 ℃, with the current of 25 mA. Then ion milling was used to clean the specimens at the voltage of 4 kV, and the current of 1 mA. Characterization of precipitated phases was performed in JEOL 200CX and 2011 TEM equipped with EDS.

3 Results and discussion

3.1 Age hardening curve and morphology

The variation in hardness as a function of ageing time is shown in Fig.1. The ageing temperatures are 150, 250 and 350 ℃, respectively. According to the time—hardness curves, one can see that the variation trend of age hardening behavior at different temperatures is quite similar. The hardness reaches peak values when the specimens are aged for about 10 h. The peak values are around Hv68, Hv70 and Hv69 corresponding to different aging temperatures, and they are comparable with many widely used Mg alloys, such as Mg-Al and Mg-Zn alloys, and the newly developed Mg-Sn-Zn alloys[14−15]. The typical microstructures of alloy after ageing at 250 ℃ are shown in Fig.2. The morphology of the precipitates has been investigated mainly when the electron beam is

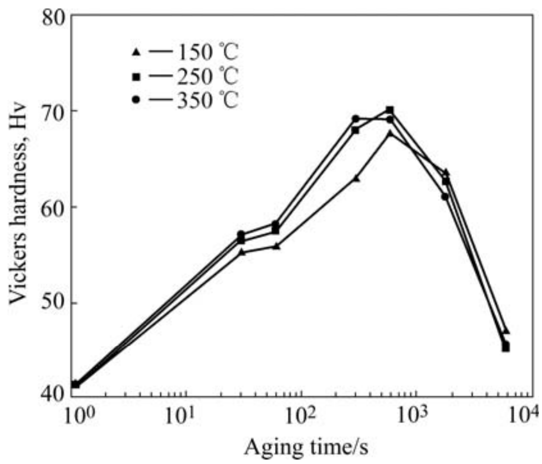

Fig.1 Age hardening response of Mg-Sn-Mn-Si alloy during ageing at 150, 250 and 350 ℃

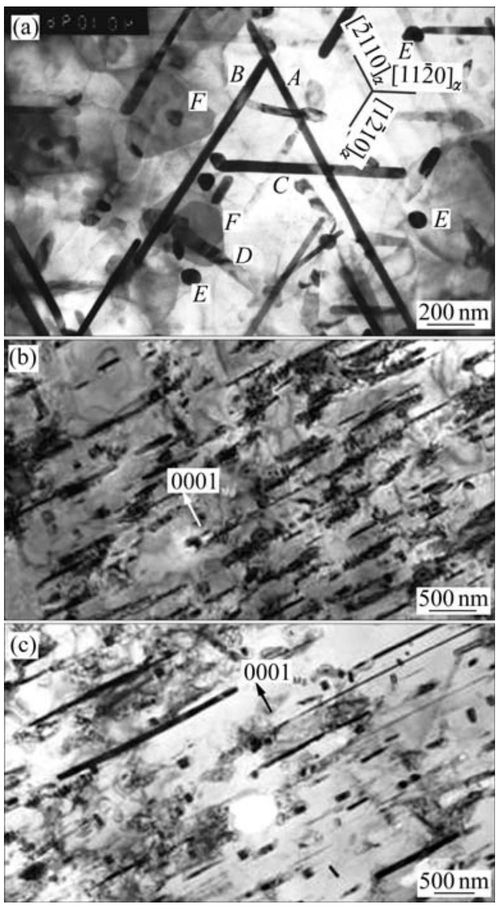

Fig.2 Microstructures of alloys after ageing at 250 ℃ for 10 h along $[0001]_\alpha$ (a), 100 h along $[2\bar{1}\bar{1}0]_\alpha$ (b) and 100 h along $[01\bar{1}0]_\alpha$

aligned parallel to three orientations of Mg matrix, i.e. $[0001]_{\alpha}$, $[2\bar{1}\bar{1}0]_{\alpha}$ and $[01\bar{1}0]_{\alpha}$. Based on the investigations we have deduced that these precipitates mainly exhibit three shapes: lath, polygon and plate. The lath shaped precipitates lie in $(0001)_{\alpha}$ plane, as labeled with *A*−*D* in Fig.2(a). The polygonal precipitates are labeled with *E* and plate-shaped precipitates are labeled with *F*. The long axis of the majority of lath precipitates is parallel to $[2\bar{1}\bar{1}0]_{\alpha}$ (*A*, *B* and *C* in Fig.2(a)). A small number of laths have their long axis along $[1\bar{1}00]_{\alpha}$ (*D* in Fig.2(a)). The polygons are almost equal-axis with about 100 nm in size (*E* in Fig.2). The plates exhibit much weaker contrast than those polygons (*F* in Fig.2), indicating that the dimension normal to $[0001]_{\alpha}$ is much smaller than that of polygons. Based on the EDS and diffraction patterns from these precipitates, we find that the majority of precipitates are Mg_2Sn phase, though a small percentage of Mn_5Si_3 and Mg_2Si have been detected.

3.2 Orientation relationships of Mg_2Sn

The majority of lath shaped Mg_2Sn exhibits the following OR: $(0001)_{\alpha}//(110)_{\beta}$, $[11\bar{2}0]_{\alpha}//[001]_{\beta}$ (OR-1). Figs.3(a), (b) and (c) show the diffraction patterns of the laths labeled with *A*, *B* and *C* in Fig.2(a), respectively. These diffraction patterns correspond to the three variants of OR-1. Many of the small diffraction spots result from double diffraction effect. Fig.3(d) shows the simulation of double diffraction effects of Fig.3(a). This OR has been reported early[10]. However, in the previous study the temperature range to form this OR was reported to be 130−200 ℃, while the present aging temperature is 250 ℃, higher than the range set previously. As seen from Fig.2(a), the angle between the long axes of the three variants of laths is 120°. The growth direction of these laths is parallel with $\langle 11\bar{2}0\rangle_{\alpha}//[001]_{\beta}$.

According to the morphology, one can see that lath-shaped precipitate *D* grows perpendicular to *B*. Its OR is different from OR-1. The diffraction pattern of precipitate *D* is shown in Fig.4. This OR can be described as: $(0001)_{\alpha}//(110)_{\beta}$, $[1\bar{1}00]_{\alpha}//[31\bar{1}]_{\beta}$ (OR-2). The long axis of *D* is parallel to $[10\bar{1}0]_{\alpha}$, as can be confirmed by the right angle between *D* and *B*, which is parallel to $[11\bar{2}0]_{\alpha}$. This OR-2 has not been reported previously. It is not certain whether this OR is due to the

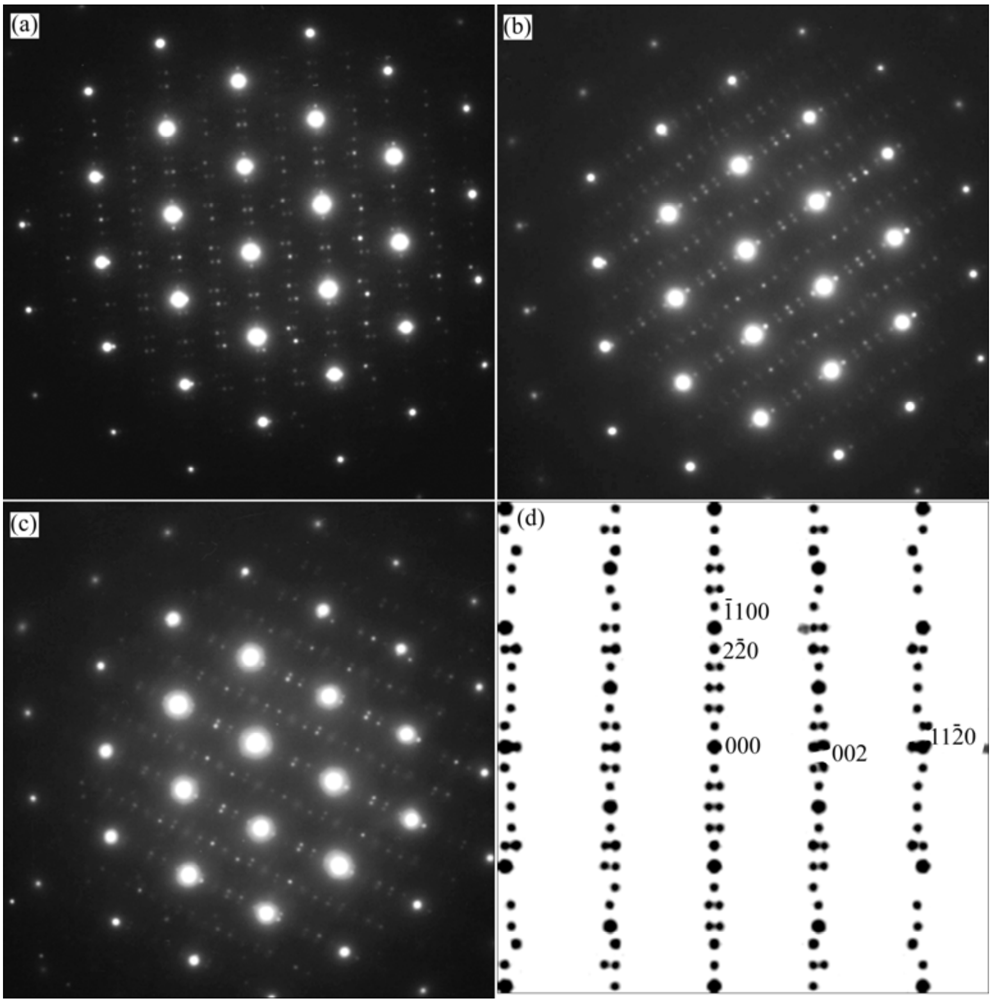

Fig.3 Diffraction pattern of *A* (a), *B* (b), *C* (c) in Fig.2 and simulation of (a) (little circles represent double diffraction spots)

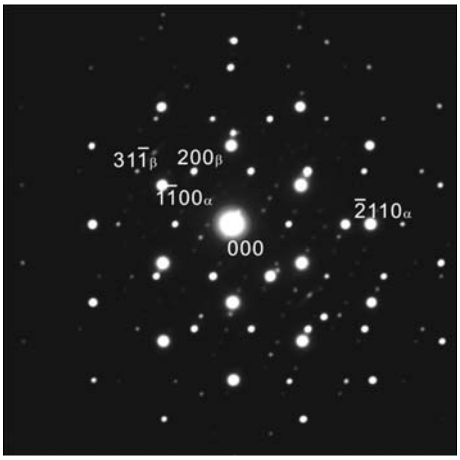

Fig.4 Diffraction pattern of lath precipitate *D* in Fig.2(a)

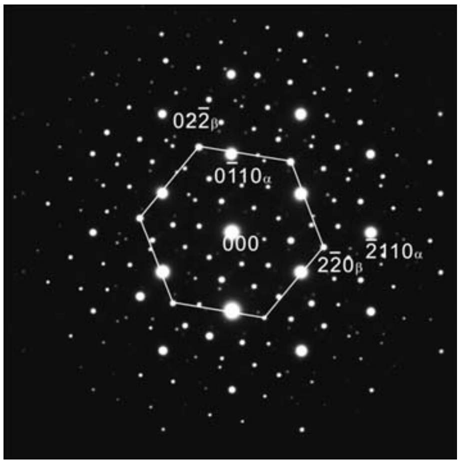

Fig.6 Diffraction pattern of plate precipitate *F* in Fig.2(a)

additions of Mn and Si, or it might be neglected in previous studies because of the similarity in morphology with OR-1, and their relative smaller amount.

Besides the lath shaped precipitates, one also finds polygonal precipitates as indicated by *E* in Fig.2. The diffraction pattern of the particle is shown in Fig.5. The OR can be described to be $[0001]_\alpha$//$[111]_\beta$, $(2\bar{1}\bar{1}0)_\alpha$ // $(\bar{1}10)_\beta$ (OR-3). The polygon precipitates are expected to have better strengthening effect compared with the lath-shapes that lie on the $(0001)_\alpha$ plane, because of their dispersive distribution and relatively larger dimension in the direction normal to $(0001)_\alpha$.

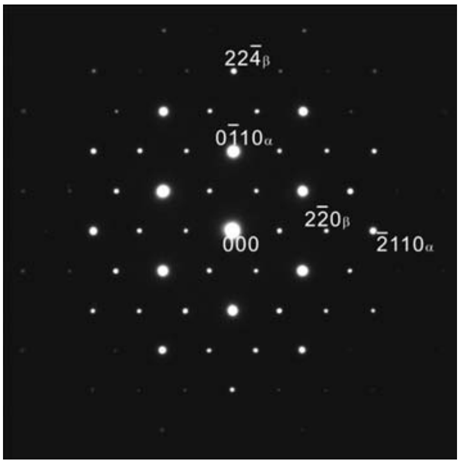

Fig.5 Diffraction pattern of polygonal precipitate *E* in Fig.2(a)

The diffraction pattern corresponding to plate-shaped precipitates is shown in Fig.6. The plates exhibit a hexagonal shape when the beam direction is parallel to $[0001]_\alpha$. Some spots in this diffraction pattern are due to double diffraction effect. Although $(0001)_\alpha$ is parallel to $(111)_\beta$ in this OR, same as OR-3, there is a rotation of about 9° around $[0001]_\alpha$//$[111]_\beta$ from OR-3. This OR can be described approximately as $(0001)_\alpha$// $(111)_\beta$; and $[2\bar{1}\bar{1}0]_\alpha$ deviates by about 9° from $[\bar{1}10]_\beta$ (OR-4). This OR has never been reported before.

The detailed analysis on Mn_5Si_3 and Mg_2Si precipitates, and the morphology of the polygonal and plate-shaped Mg_2Sn precipitates will be presented elsewhere.

4 Conclusions

The crystallography of Mg_2Sn precipitates in a Mg-Sn-Mn-Si alloy was reported. The Mg_2Sn precipitates mainly exhibit three shapes: lath, polygon and plate. Most of the lath shaped Mg_2Sn precipitates exhibit the ORs of OR-1 and OR-2 as described; polygonal Mg_2Sn precipitates exhibit OR-3; and plate-shaped precipitates exhibit OR-4. Among the four kinds of ORs, OR-1 and OR-3 have been reported in literature; OR-2 and OR-4, together with the corresponding morphology, are newly observed. The addition of Mn and Si promotes the formation of polygonal Mg_2Sn precipitates, which possibly have better strengthening effect than lath shaped Mg_2Sn.

Acknowledgements

The authors would like to thank Dr. ZHENG Wei-chao, Mr. HUANG Bing-yuan and Mr. ZHAO Qing-long for their assistant in preparing the alloys.

References

[1] POLMEAR I J. Overview: Magnesium alloys and applications [J]. MSEA, 1994, 10: 1−16.

[2] LUO A. Magnesium castings for automotive applications [J]. JOM, 1995, 47: 28−31.

[3] LEE J Y, DO H K, LIM H K, KIM D H. Effects of Zn/Y ratio on microstructure and mechanical properties of Mg-Zn-Y alloys [J]. Materials Letters, 2005, 59: 3801−3805.

[4] LUO Z P, SONG D Y, ZHANG S Q. Strengthening effects of rare-earths on wrought Mg-Zn-Zr-RE alloys [J]. J Alloys Compd, 1995, 230(2): 109−114.

[5] UNSWORTH W, KING J F. Magnesium technology [M]. London: Institute of Metals, 1987.

[6] OH J C, OHKUBO T, MUKAI T, HONO K. TEM and 3DAP characterization of an age-hardened Mg-Ca-Zn alloy [J]. Scripta Mater, 2005, 53(6): 675−679.

[7] WEI L Y, DUNLOP G L, WESTENGEN H. Age hardening and precipitation in a cast magnesium rare-earth alloy [J]. J Mater Sci, 1996, 31(2): 387−397.

[8] YAMASHITA T, KELLY P M, CAVALLARO P, HISA M. Effects of age hardening of magnetic and transport properties of Mg-1.3% Ce alloys [J]. Acta Mater, 1998, 46(9): 2977−2981.

[9] NIE J F, MUDDLE B C. Characterization of strengthening precipitate phases in a Mg-Y-Nd alloy [J]. Acta Mater, 2000, 48: 1691−1703.

[10] HENES S, GEROLD V. Roentgenographic investigation of the separation processes in magnesium-lead and magnesium-zinc alloys [J]. Z Metallk, 1962, 53: 743−751.

[11] PLANKEN J. Precipitation hardening in magnesium-tin alloys [J]. J Mater Sci Lett, 1969, 4: 927−929.

[12] NIE J F. Effects of precipitate shape and orientation on dispersion strengthening in magnesium alloys [J]. Scripta Mater, 2003, 48(8): 1009−1015.

[13] KANG D H, PARK S S, OH Y S, KIM N J. Effect of nano-particles on the creep resistance of Mg-Sn based alloys [J]. MSEA, 2007, 449: 318−321.

[14] SASAKI T T, OHISHI K, OHKUBO T, HONO K. Enhanced age hardening response by the addition of Zn in Mg-Sn alloys [J]. Scripta Mater, 2006, 55(3): 251−254.

[15] MENDIS C L, BETTLES C J, GIBSON M A, HUTCHINSON C R. An enhanced age hardening response in Mg-Sn based alloys containing Zn [J]. MSEA, 2006, 435: 163−171.

[16] LIU H M, CHEN Y G, TANG Y B, HUANG D M, TU M J, ZHAO M, LI Y G. Effect of Zr-adding on microstructure and mechanical properties for Mg-5Sn alloy [J]. Rare Metal Materials and Engineering, 2006, 35(12): 1912−1915.

[17] HORT N, HUANG Y D, ABU L T, MAIER P, KAINER K U. Microstructural investigations of the Mg-Sn-xCa system [J]. Adv Eng Mater, 2006, 8(5): 359−364.

[18] BAMBERGER M. Phase formation in Mg-Sn-Zn alloys—thermodynamic calculations vs experimental verification [J]. J Mater Sci, 2006, 41(10): 2821−2829.

[19] KANG D H, PARK S S, KIM N J. Development of creep resistant die cast Mg-Sn-Al-Si alloy [J]. MSEA, 2005, 413: 555−560.

[20] BOWLES A L, DIERINGA H, BLAWERT C, HORT N, KAINER K U. Investigations in the magnesium-tin system [J]. Materials Science Forum, 2005, 488/489: 135−138.

(Edited by YANG Bing)